Heavy metal incorporated helium ion active hybrid non-chemically amplified resists: Nano-patterning with low line edge roughness

Cite as: AIP Advances **7**, 085314 (2017); https://doi.org/10.1063/1.4989981
Submitted: 13 June 2017 • Accepted: 10 August 2017 • Published Online: 22 August 2017

Pulikanti Guruprasad Reddy, Neha Thakur, Chien-Lin Lee, et al.

Heavy metal incorporated helium ion active hybrid non-chemically amplified resists: Nano-patterning with low line edge roughness

Pulikanti Guruprasad Reddy,[1,a] Neha Thakur,[1,a] Chien-Lin Lee,[2] Sheng-Wei Chien,[2] Chullikkattil P. Pradeep,[1,b] Subrata Ghosh,[1,b] Kuen-Yu Tsai,[2,b] and Kenneth E. Gonsalves[1,b]
[1]*School of Basic Sciences, Indian Institute of Technology Mandi, Kamand 175005, Himachal Pradesh, India*
[2]*Department of Electrical Engineering, National Taiwan University, Taipei 10617, Taiwan*

(Received 13 June 2017; accepted 10 August 2017; published online 22 August 2017)

Helium (He) ion lithography is being considered as one of the most promising and emerging technology for the manufacturing of next generation integrated circuits (ICs) at nanolevel. However, He-ion active resists are rarely reported. In this context, we are introducing a new non-chemically amplified hybrid resist (n-CAR), MAPDSA-MAPDST, for high resolution He-ion beam lithography (HBL) applications. In the resist architecture, 2.15 % antimony is incorporated as heavy metal in the form of antimonate. This newly developed resists has successfully used for patterning 20 nm negative tone features at a dose of 60 μC/cm^2. The resist offered very low line edge roughness (1.27±0.31 nm) for 20 nm line features. To our knowledge, this is the first He-ion active hybrid resist for nanopatterning. The contrast (γ) and sensitivity (E_0) of this resist were calculated from the contrast curve as 0.73 and 7.2 μC/cm^2, respectively. [http://dx.doi.org/10.1063/1.4989981]

I. INTRODUCTION

In the semiconductor industries, patterning feature size down at 10 nm node is highly dependent on the advancements in lithography patterning techniques and capability of the photoresist used.[1–6] Electron beam lithography (EBL) has been developed long ago and it has enabled fabrication of features with sub-10 nm pitch for industrial as well as academic research applications.[6,7] However, backscattering and the subsequent secondary electrons induced proximity effect in e-beam patterning process eventually affects the high resolution feature nodes particularly at sub-10 nm level.[8] Therefore, to overcome this issue, researchers have developed He-ion beam microscope for performing He-ion beam lithography (HBL) as an alternative patterning technique for higher resolution (sub-10 nm) lithography applications.[9–12] He-ion beam uses smaller de-Broglie's wavelength (higher momentum) which results in high resolution, high contrast and reduced proximity effect as compared to the EBL.[9–12] Previous reports on the He-ion beam lithography breakthrough into the sub-10 nm regime with enhanced sensitivity and resolutions than the performance compared to e-beam achievements.[13,14] Therefore, the design of high resolution features under He-ion beam conditions are the dire need for the next generation ICs manufacturing.

Moreover, for He-ion lithography resists, thin films require sub-40 nm thickness for the development of collapse free patterns at higher resolution nodes.[8] However, due to the risk of structure loss during development and rinsing process at lower thickness, patterning of such features with higher

[a]Both the Authors have contributed equally to this work.
[b]Corresponding authors: pradeep@iitmandi.ac.in; subrta@iitmandi.ac.in; ktsai@ntu.edu.tw, kenneth@iitmandi.ac.in

FIG. 1. Chemical structures of the 2.15 %-MAPDSA-MAPDST copolymer resist.

aspect ratio is a challenging task. Design of newer resist structures with required characteristics is one of the possible solution for the above issues. Literature reports on He-ion active resists are very rare as compared to other patterning techniques that include EBL, EUVL and 193 nm immersion lithography etc. Till date, two commercial electron beam active resists i.e. PMMA and HSQ have been utilized extensively as the resist materials for the patterning of nano features under He-ion beam conditions.[13,14] In addition, Shi *et. al*. reported fullerene based negative tone molecular resist for sub-10 nm patterning applications at the dose ~ 40 μC/cm^2.[8] Similarly, Zhou *et. al.* fabricated 5 nm half-pitch arrays of graphene nano ribbons under He-ion beam conditions with lower beam spot size at 4 nm.[15] Moreover, HafSOx inorganic resist came into the existence for the He-ion beam applications with enhanced dose characteristics than the similar resist analyzed under EBL.[16] Therefore, a careful literature survey reveals that the development of He-ion active resists is highly desirable for futuristic technological nodes.

Trifluoromethane sulfonate (triflate) functionality has been utilized extensively in developing resist materials for a wide range of lithography tools (EUV, EBL and immersion lithography techniques), for patterning various nodes starting from higher to lower nodes.[2,17–20] However, their sensitivity toward He-ion beam radiations has not been explored yet. In this regard, by the copolymerization of aromatic sulfonium triflate monomer (MAPDST) with antimony containing monomer (MAPDSA), we have successfully developed a hybrid copolymer resist MAPDSA-MAPDST containing 2.15% MAPDSA for high resolution He-ion beam lithography applications (See, FIG 1). The radiation sensitive MAPDST unit was incorporated into final hybrid resist structure due to its ability to bring polarity changes by conversion of hydrophilic sulfonium functionality into hydrophobic sulfide functionality during lithography process.[17] Due to synergistic interactions between the organic and inorganic units which result in an enhanced properties like sensitivity, adhesion, resolution and etch resistance than pure organic resist thin films, organic-inorganic hybrid resists have attracted the immense attention in the field of lithography.[21–24] Our previous EUVL studies on 2.15%-MAPDSA-MAPDST hybrid resist thin films have revealed that the small percentage of inorganic SbF_6 component in the resist structures helps to improve the overall sensitivity than pure poly-MAPDST homopolymer.[25] Therefore, given that there is no report on hybrid resists for HIBL, we investigated the potential of this particular hybrid composition for patterning nano features using HIBL. The designed resist has shown 20 nm (line/4space, L/4S) sharp features with bright contrast, high sensitivity and very low LER values. The details of the lithography studies are presented in later sections.

II. MATERIALS AND METHODS

A. Materials

The hybrid copolymer resist 2.15%-MAPDSA-MAPDST was synthesized according to our previously published protocol by copolymerization of organic monomer MAPDST (4-(methacryloyloxy)phenyldimethylsulfoniumtriflate) and hybrid inorganic monomer MAPDSA

(4-(methacryloyloxy)phenyl dimethylsulfoniumhexaflouroantimonate) in the presence of azobisisobutyronitrile (AIBN) as a free radical initiator under N_2 atmosphere for 2 days.[25] All the characterization data obtained from FT-IR, NMR and gel permeation chromatography (GPC) were in well accordance with the literature data.[25] Figure 1 shows the chemical structure of MAPDSA-MAPDST copolymer resist, where x and y represent different chemical composition of MAPDSA (2.15%) and MAPDST (97.85%) units in the copolymer resist respectively. HPLC grade Acetonitrile (99.99%) and tetramethylammonium hydroxide (TMAH) were purchased from commercial source and used as received.

B. Thin film preparation and He-ion beam assessment

The resist solution was prepared by dissolving of solid 2.15%-MAPDSA-MAPDST polymer in acetonitrile solution followed by filtration through 0.2 μm Teflon filter in order to remove undissolved particles. The resist thin film with ~40 nm thickness was achieved by spin coating of resist solutions on 2″ p-type silicon substrate at 4500 rpm speed for 60 sec. Thereafter, thin films were pre-baked at 60 °C for 60 sec and then subjected to He-ion beam exposures source for the nanofabrication using ZESISS Orion Nano Fab He-ion microscope at National Taiwan University. Prior to He-ion bombardment, the ion beam was aligned using a current of 0.5 pA. With 10 μm aperture, the He beam (at an acceleration of 30 KV with a beam current of 0.5 pA) was operated while keeping the dwell time constant at 0.1 μs and beam spacing of 1 nm. Considering it as a matrix of 100 blocks (10*10), the initial dose for block 1 was 50 μC/cm^2 and with each block it was increased by a step of 10 μC/cm^2 up to dose of 1040 μC/cm^2 (See, FIG. 2). Each block was having pattern of 10 lines of 20 nm with L/4S characteristics. After exposure to highly energetic He-ion beam at certain dose, post exposure bake (60 °C for 60 sec) was applied to the exposed thin film which helps in completion of the chemical reactions induced by ion beam. The solubility property was altered through transformation in functionality from polar Ar-S$^+$-$(CH_3)_2$ into non-polar Ar-S-CH_3 sulfide entity.[26] Since the interaction between the developer and resist greatly defines the LER of resist, developing conditions certainly require optimization. For optimization various experiments were carried out with different concentration of TMAH and it was concluded that use of 0.022N TMAH as developer for 15 sec delivered us the best results while use of 0.262 N TMAH (industry standard) directly results in washing-off the both exposed and unexposed area within 5 sec.

C. Helium ion microscope (HIM) and AFM characterization details

ZESISS Orion He-ion microscope and Atomic Force Microscope (Veeco Dimension, integrated with the Olympus OMCL-AC160TS cantilever tip) were utilized for investigating the

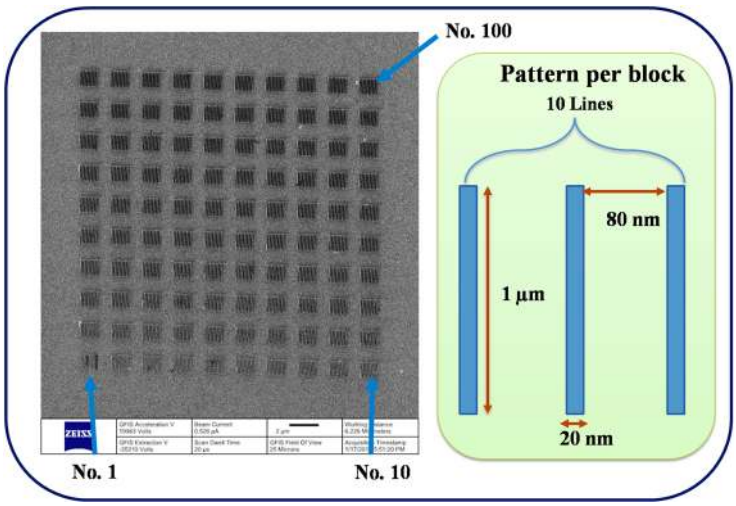

FIG. 2. Dose test on spin coated 2.15 %-MAPDSA-MAPDST resist thin film (Dose: 50-1040 μC/cm^2).

critical dimensions (CD) of the line features obtained from the 2.15%-MAPDSA-MAPDST resist.

III. RESULTS AND DISCUSSIONS

To find the optimum exposure dose, 2.15%-MAPDSA-MAPDST resist coated thin films were exposed to He-ion beam radiations in the range from 50-1040 μC/cm^2 (See, FIG. 2). The dose test analyses reveal that 60 μC/cm^2 is the minimum exposure dose that the resist film required to change polarity of the exposed area as compared to unexposed area and for patterning 20 nm line features after TMAH development. However, this particular dose is also not prominent to achieve the defect free patterns at nano level (See, FIG 3b). The 20 nm line features with L/4S (line/space) characteristics obtained from the 2.15%-MAPDSA-MAPDST resist at He-ion doses 50, 60, 340 and 540 μC/cm^2 are presented in FIG. 3 (a–d) respectively. There is discontinuity of the resist line features observed in the case of FIG. 3 a, b. This is due to loss of resist structures because of under-exposure of resist thin films at the given experimental conditions. However, the pattern collapse behaviour of this resist could be controlled by tuning the exposure dose. For example, pattern collapse could be avoided in the case of 20 nm line features when these nano features were patterned at higher doses such as 110 μC/cm^2

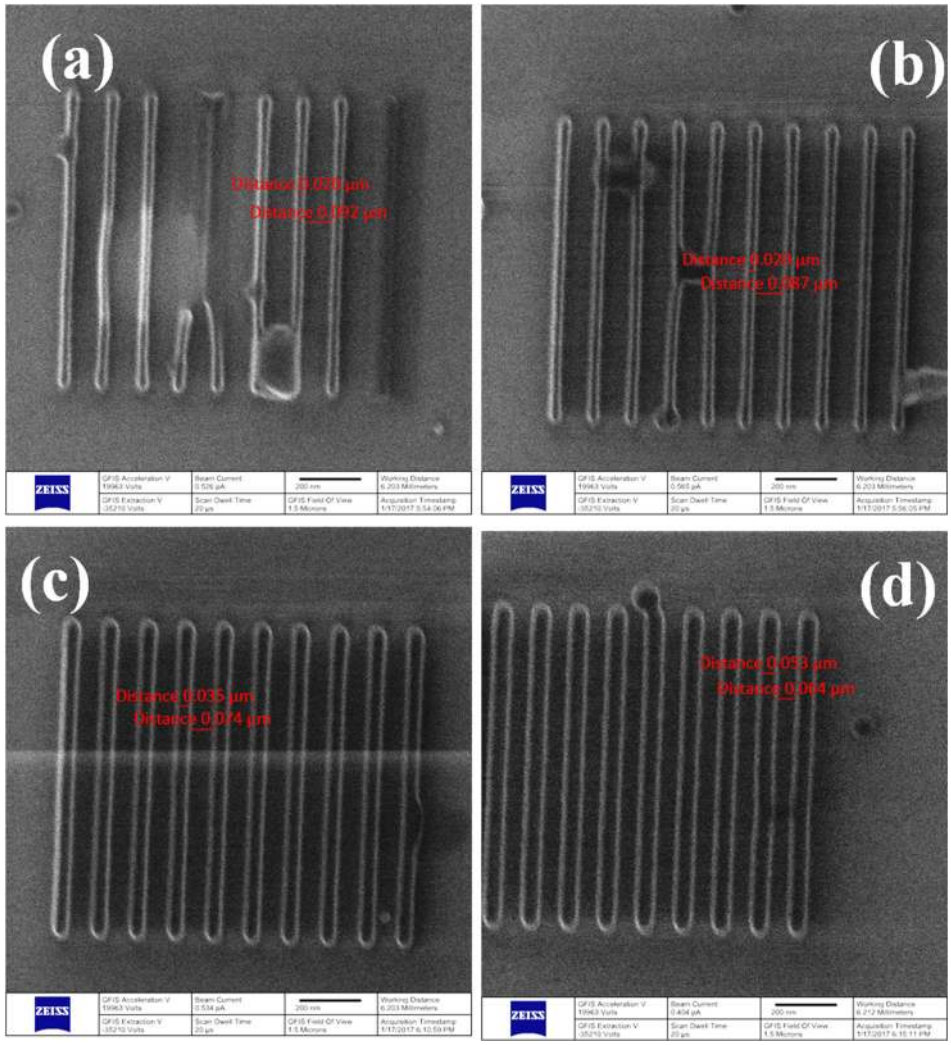

FIG. 3. 20 nm (L/4S) line features of the 2.15 %-MAPDSA-MAPDST resist at various doses: (a) 50 μC/cm^2, (b) 60 μC/cm^2, (c) 340 μC/cm^2, and (d) 540 μC/cm^2.

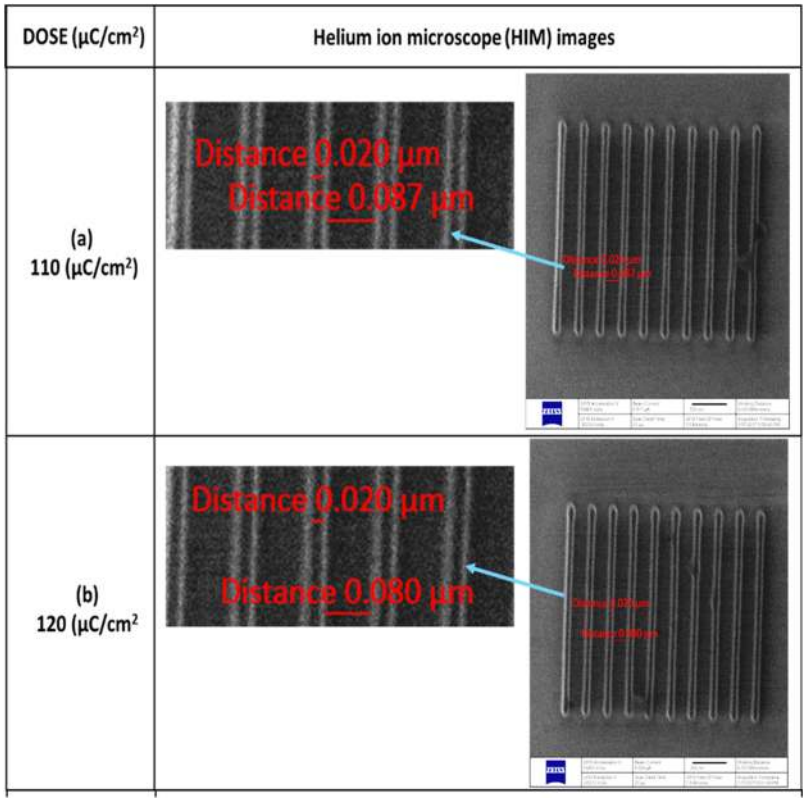

FIG. 4. He-ion exposed 20 nm (L/4S) line patterns of 2.15%-MAPDSA-MAPDST resist (100X magnification): a) At a dose 110 μC/cm^2, b) At a dose 120 μC/cm^2.

and 120 μC/cm^2 as shown in FIG. 4 (a–b). However, the efforts to achieve lower node features at sub-10 nm regime using synthesized 2.15 %-MAPDSA-MAPDST were unsuccessful which probably corresponds to the resolution limit of the resist.

Interestingly, it has been observed that the critical dimensions (CD) of the resist features were increasing continuously with the exposure dose. For example, the hybrid resist patterns obtained at doses 340 and 540 μC/cm^2 (FIG 3 c–d), revealed that actual (20 nm) CD of patterned features appeared to be 35 and 53 nm respectively. It was attributed to increase in the number of backscattered electrons which interacted with large exposure area of the resist thin film and resulted in high CD patterns.

To view the line patterns topography, the HIM stage was tilted to 45 ° and based on this sample geometry, the effective thickness of the line features were measured (See, FIG. 5). The magnified cross sectional view of 20 nm line features with L/4S (line/space) characteristics was shown in the FIG. 6a. The line edge roughness (LER) of these features was calculated using a standard metrology analysis tool of the "SUMMIT" package as 1.27±0.31 nm which was found to be better than He-ion resists reported in the literature.[8] The synthesized hybrid resist offered us low LER (1.27±0.31 nm) in comparison to other reported traditional resists[8] and results in well resolved, collapse free and nano-smooth lines with high imaging contrast (See, FIG. 6). The line thickness was measured from HIM tilted images and found as ~40 nm, which was similar to the thickness (~ 40 nm) as found for pre-exposure resist film. This indicated no resist loss during lithography process at a dose 110 μC/cm^2 (See, FIG 6b). Furthermore, using AFM tool, the obtained resist line features were characterized. Radius curvature of tip apex of 7 nm and cantilever spring constant of 26 N/m were used for the AFM analysis. The AFM topography of well resolved negative patterns (20 nm features with L/4S characteristics) of 2.15%-MAPDSA-MAPDST are shown in FIG. 7.

The AFM images also revealed no left over resists in the trenches after developing and the negative tone patterns are well developed with very sharp edges. In important to note that no deformation

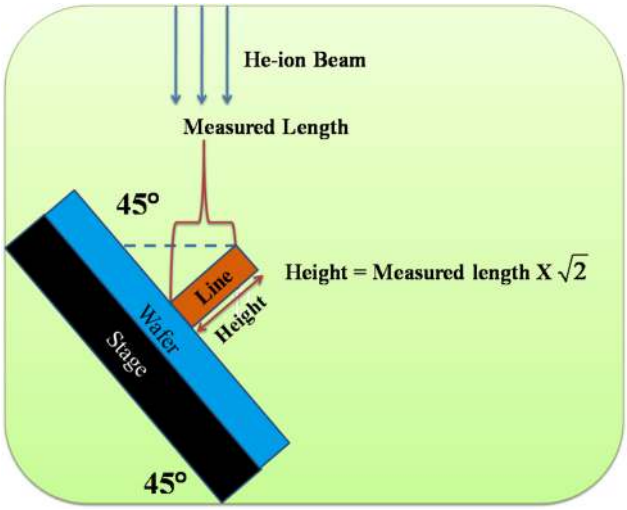

FIG. 5. Schematic presentation of tilting HIM stage at 45 ° for calculating 20 nm lines thickness.

of patterns was noticed during AFM imaging indicating very good adhesion between this He-ion active resists and the silicon substrate. This is one of the most important requirements for any newly developed resists to be used for semiconductor industries.

In order to estimate the contrast (γ) and sensitivity (E_o), the He-ion induced 2.15%-MAPDSA-MAPDST patterns were computed to normalized remaining thickness (NRT) analyses. In general, NRT curve provides the information about the quality of the resist. The residual thickness of the 2.15%-MAPDSA-MAPDST resist was plotted as a function of varying He-ion exposure doses as shown in FiG. 8. The exposure doses starting from 1-50 $\mu C/cm^2$ were considered for the sensitivity curve analysis and the obtained residual thickness of resist features were measured using AFM analyses. The resist thin films exposed at doses 1 and 2 $\mu C/cm^2$, seems to have no residual thickness of the resist on the silicon substrate, while in the case of doses 3-5 $\mu C/cm^2$, the resist was found to have a shallow thickness with a low contrast. This observation reveals that the given dose characteristics are inadequate to bring the change in polymer polarity. In contrast, the observed thicker resist features at dose ≥ 10 $\mu C/cm^2$ suggested that resists thin film experience full exposure under the

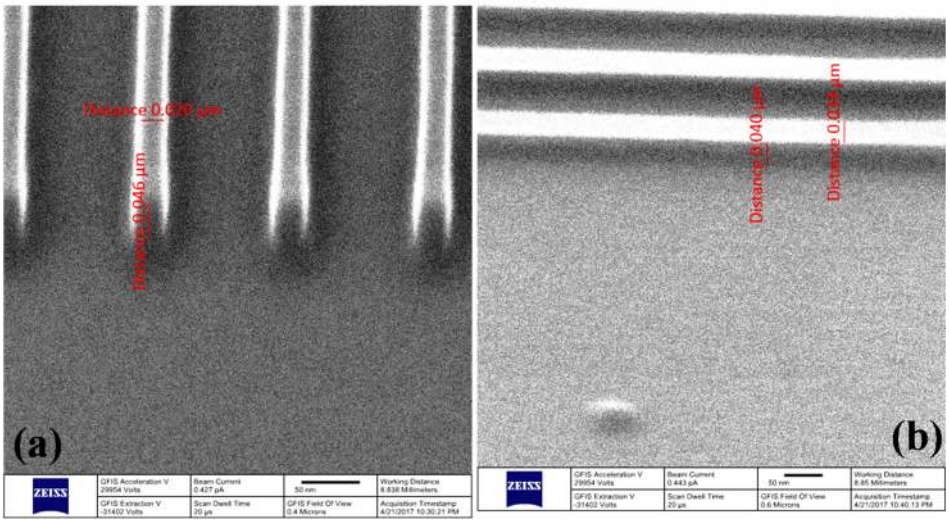

FIG. 6. a) Cross sectional view of 20 nm (L/4S) features at a dose 110 $\mu C/cm^2$ (Magnification: 300X), b) Thickness measurements of 20 nm line features by tilting the line patterns at 45° angle (Magnification: 200 X, Dose: 110 $\mu C/cm^2$).

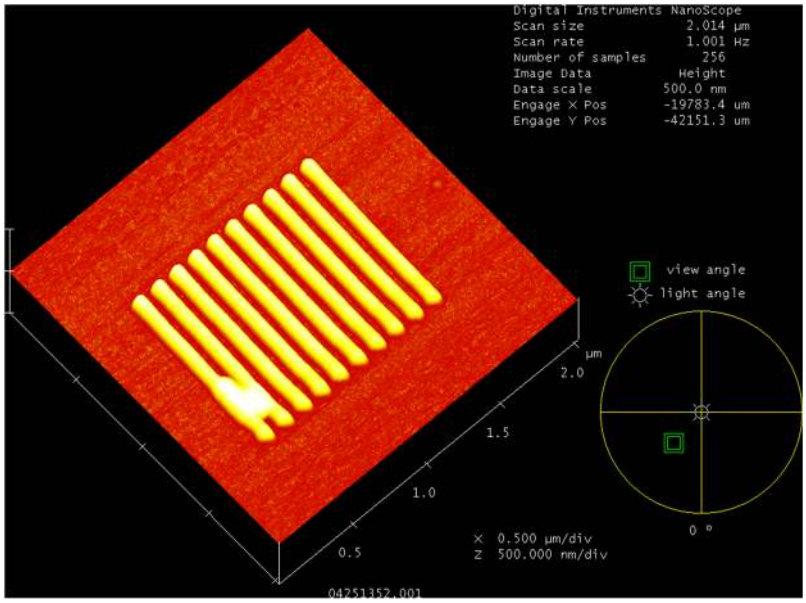

FIG. 7. AFM topography of 20 nm (L/4S) line features of the 2.15%-MAPDSA-MAPDST resist at the dose 110 μC/cm^2.

given He-ion beam conditions (See, FIG. 9). This image analyses reveal that the residual thickness of the resist features increased gradually with the exposure dose, which represent the negative tone nature of the resist formulations. The calculated γ and E_o for the developed hybrid resist formulations were 0.73 and 7.2 μC/cm^2 respectively (See, FIG. 8). The sensitivity (7.2 μC/cm^2) of the resist was found to be better than many of the reported He-ion beam resists.[8,13,27] However, the minimum exposure dose for He-ion beam required to achieve 20 nm line features is 60 μC/cm^2. For analysing dose characteristics, the experiments were performed at micro level[8] aiming towards concluding the minimum dose required for inducing the change in structure of resist as shown in Fig. 9. Thus after NRT curve was used to calculate the sensitivity and found to be 7.2 μC/cm^2. The present resist is not utilizing any photoactive compounds like photoacid generator (PAG) for their structural transformations, indicating that the current resist acts as a non-chemically amplified resist.

As discussed above, sulfonium triflates are sensitive toward light and radiations.[17–20] There are well known mechanisms for these sulfonium based resists which interact with the high energy photons

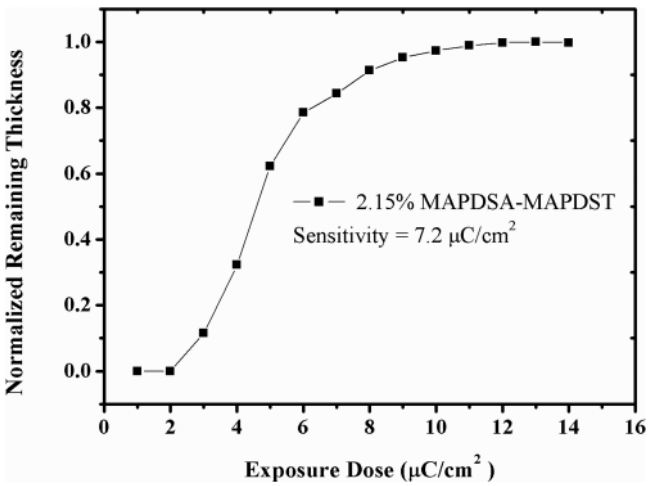

FIG. 8. NRT vs He-ion dose characteristics of the 2.15%-MAPDSA-MAPDST resist.

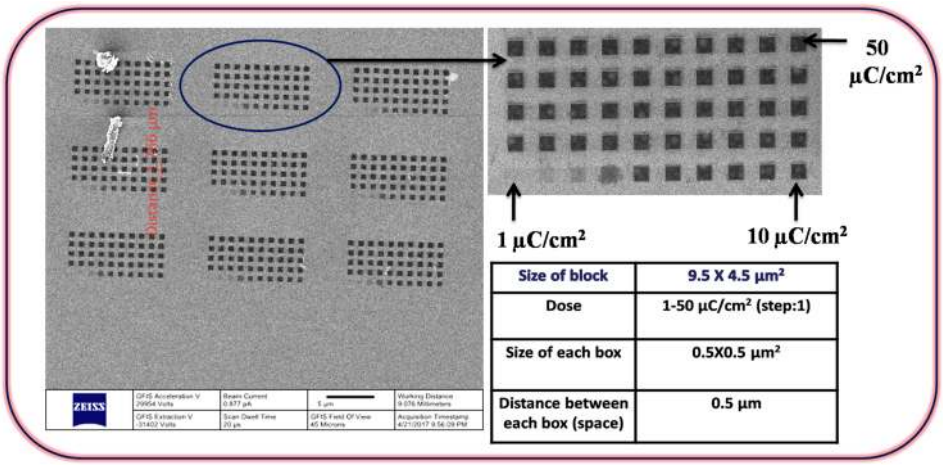

FIG. 9. Analysed dose characteristics (1-50 μC/cm^2) for NRT curve analyses.

or radiation source and undergo photochemically induced conversion into sulfide functionality.[28] Hence, this induced structural change leads to the change in polarity from the hydrophilic sulfonium to hydrophobic sulfide.[28] Hence, the hydrophilic 0.02N TMAH (used as the developer) dissolved the hydrophilic unexposed area and resulted in negative tone patterning on the silicon substrate. It was clearly observed by looking at the images taken from HIM that the exposed region of hybrid resists remained on the surface of silicon substrate while the unexposed region was washed away.

IV. CONCLUSIONS

In summary, we have demonstrated the potential of hybrid non-chemically amplified resist, 2.15%-MAPDSA-MAPDST, based on the radiation sensitive organic monomer MAPDST and inorganic hybrid monomer MAPDSA for He-ion beam lithography applications. To our knowledge, this is the first hybrid resist reported so far for HIBL applications. We have been successful in patterning 20 nm line features with L/4S characteristics using HIBL technique and the patterns were characterized by higher resolution HIM and AFM tools. The worth mentioning characteristics of these nano features are their low LER (1.27±0.31 nm) which is better than the reported He-ion resists. The contrast and sensitivity of the resist were calculated from the sensitivity curve as 0.73 and 7.2 μC/cm^2 respectively. AFM analysis clearly revealed well developed pattern with sharp inner walls and good adhesion of the patterns with the silicon surface. Based on all these experimental outcomes, we strongly believe that the present experimental findings can provide a basic idea to wide audience for the development of new He-ion active resists in the field of futuristic lithography applications.

ACKNOWLEDGMENTS

We thank Department of Science and Technology (DST), India and Ministry of Science and Technology (MOST), Taiwan for financial support; Project reference numbers GITA/DST/TWN/P-69/2015 and MOST/104-2923-E-002-007-MY3. National Synchrotron Radiation Research Centre (NSRRC), Taiwan and Instrument Technology Research Centre of National Applied Research Laboratories, Taiwan are gratefully acknowledged for facility support. P. G. Reddy thanks to the Council of Scientific and Industrial Research (CSIR), India for senior research fellowship.

[1] H. P. Alesso and C. F. Smith, *Connections: patterns of discovery*, John Wiley & Sons, New Jersey, (2008).
[2] S. Ghosh, C. P. Pradeep, S. K. Sharma, P. G. Reddy, S. P. Pala, and K. E. Gonsalves, RSC Adv. **6**, 74462 (2016).
[3] R. F. Pease and S. Y. Chou, Proc. IEEE **96**, 248 (2008).
[4] N. Mojarad, M. Hojeij, L. Wang, J. Gobrecht, and Y. Ekinci, Nanoscale **7**, 4031 (2015).
[5] B. Wu and A. Kumar, J. Vac. Sci. Technol. B **25**, 1743 (2007).
[6] A. S. Gangnaik, Y. M. Georgiev, and J. D. Holmes, Chem. Mater. **29**, 1898 (2017).
[7] J. K. W. Yang, B. Cord, H. Duan, K. K. Berggren, J. Klingfus, S. W. Nam, K. B. Kim, and M. J. Rooks, J. Vac. Sci. Technol. B. **27**, 2622 (2009).

[8] X. Shi, P. Prewett, E. Huq, D. M. Bagnall, A. P. G. Robinson, and S. A. Boden, Microelectron. Eng. **155**, 74 (2016).
[9] M. T. Postek, A. Vladár, C. Archie, and B. Ming, Meas. Sci. Technol. **22**, 024004 (2011).
[10] M. T. Postek and A. E. Vladár, Scanning **30**, 457 (2008).
[11] L. Scopioni, C. A. Sanford, J. Notte, B. Thompson, and S. McVey, J. Vac. Sci. Technol. B. **27**, 3250 (2009).
[12] G. Hlawacek, V. Veligura, R. V. Gastel, and B. Poelsema, J. Vac. Sci. Technol. B. **32**, 020801 (2014).
[13] V. Sidorkin, E. V. Veldhoven, E. V. Drift, P. Alkemade, H. Salemink, and D. Maas, J. Vac. Sci. Technol. B. **27**, L18 (2009).
[14] D. Winston, B. M. Cord, B. Ming, D. C. Bell, W. F. DiNatale, L. A. Stern, A. E. Vladar, M. T. Postek, M. K. Mondol, J. K. W. Yang, and K. K. Berggren, J. Vac. Sci. Technol. B **27**, 2702 (2009).
[15] A. N. Abbas, G. Liu, B. Liu, L. Zhang, H. Liu, D. Ohlberg, W. Wu, and C. Zhou, ACS Nano **8**, 1538 (2014).
[16] F. Luo, V. Manichev, M. Li1, G. Mitchson, B. Yakshinskiy, T. Gustafsson, D. Johnson, and E. Garfunkel, Proc. SPIE. **9779**, 977928 (2016).
[17] P. G. Reddy, S. P. Pal, P. Kumar, C. P. Pradeep, S. Ghosh, S. K. Sharma, and K. E. Gonsalves, ACS Appl. Mater. Interfaces **9**, 17 (2017).
[18] V. Singh, V. S. V. Satyanarayana, S. K. Sharma, S. Ghosh, and K. E. Gonsalves, J. Mater. Chem. C **2**, 2118 (2014).
[19] K. Gonsalves, L. Merhari, H. Wu, and Y. Hu, Adv. Mater. **13**, 703 (2001).
[20] M. Wang, N. D. Jarnagin, C. T. Lee, C. L. Henderson, W. Yueh, J. M. Roberts, and K. E. Gonsalves, J. Mater. Chem. **16**, 3701 (2006).
[21] R. D. Re, J. Passarelli, M. Sortland, B. Cardineau, Y. Ekinci, E. Buitrago, M. Neisser, D. A. Freedman, and R. L. Brainard, J. Micro/Nanolith. MEMS MOEMS **14**, 043506 (2015).
[22] M. Sortland, J. Hotalen, R. D. Re, J. Passarelli, M. Murphy, T. S. Kulmala, Y. Ekinci, M. Neisser, D. A. Freedman, and R. L. Brainard, J. Micro/Nanolith. MEMS MOEMS **14**, 043511 (2015).
[23] W. J. Bae, M. Trikeriotis, J. Sha, E. L. Schwartz, R. Rodriguez, P. Zimmerman, E. P. Giannelis, and C. K. Ober, J. Mater. Chem. **20**, 5186 (2010).
[24] K. Kasahara, H. Xu, V. Kosma, J. Odent, E. P. Giannelis, and C. K. Ober, Proc. SPIE **10143**, 1014308 (2017).
[25] K. E. Gonsalves, S. Ghosh, C. P. Pradeep, G. P. Reddy, S. K. Sharma, and P. Kumar, Indian Pat. Appl. IN 2016-11022219.
[26] V. Singh, V. S. V. Satyanarayana, N. Batina, I. M. Reyes, S. K. Sharma, F. Kessler, F. R. Scheffer, D. E. Weibel, S. Ghosh, and K. E. Gonsalves, J. Micro/Nanolith. MEMS MOEMS **13**, 043002 (2014).
[27] E. van der Drift and D. J. Maas, *Helium ion lithography* (Springer, 2012).
[28] G. R. Chagas, V. S. V. Satyanarayana, F. Kessler, G. K. Belmonte, K. E. Gonsalves, and D. E. Weibel, ACS Appl. Mater. Interfaces **7**, 16348 (2015).